

A DEEP EXTREME ULTRAVIOLET EXPLORER OBSERVATION OF THE EXTREME ULTRAVIOLET TRANSIENT RE J1255+266

JEREMY J. DRAKE AND ANTONELLA FRUSCIONE

Harvard-Smithsonian Center for Astrophysics, MS-3, 60 Garden Street, Cambridge, MA 02138;
 jdrake@cfa.harvard.edu, antonell@cfa.harvard.edu

MELVIN G. HOARE

Department of Physics and Astronomy, University of Leeds, Leeds, LS2 9JT, England, UK; mgh@ast.leeds.ac.uk

AND

PAUL CALLANAN

Department of Physics, University College Cork, Ireland; paulc@ucc.ie

Received 1997 June 12; accepted 1997 September 9

ABSTRACT

We report on the analysis of a deep *Extreme Ultraviolet Explorer* (*EUVE*) observation made with the Deep Survey and Spectrometer telescope, which included in the field the remarkable bright extreme ultraviolet (EUV) transient source RE J1255+266, discovered in 1994 June by the *ROSAT* Wide Field Camera (WFC). A careful analysis of the resulting Deep Survey (DS) Lexan/B (67–178 Å) image, whose aggregated exposure time is 137 ks, has not revealed any trace of the source but has yielded a quite stringent formal upper limit on the quiescent *EUVE* DS count rate of 0.003 counts s⁻¹ (3 σ) and a “visual” upper limit of 0.002 counts s⁻¹. An analysis based on blackbody spectra, pure hydrogen DA white dwarf models, and optically thin plasma model spectra has provided constraints on the source counterpart. The observed count rate upper limit is consistent with the optical identification proposed by Watson et al. in which a DA white dwarf is the primary component of a CV-like system involving a very low mass M dwarf secondary star. Our upper limit to the *EUVE* DS count rate, when compared with the count rate observed with the *ROSAT* WFC at the peak of the outburst, implies a brightening of the EUV source flux relative to quiescence by a factor of greater than 54,000.

Subject headings: binaries: close — novae, cataclysmic variables — ultraviolet: stars — X-rays: bursts

1. INTRODUCTION

The bright extreme ultraviolet (EUV) transient source RE J1255+266 was detected serendipitously in a *ROSAT* Wide Field Camera (WFC) observation toward the Coma cluster of galaxies carried out in 1994 June–July (Dahlem & Kreysing 1994; Dahlem et al. 1995). Dahlem et al. (1995) reported an EUV flux in the 62–110 eV (112–200 Å) band (WFC S2 filter; Pounds et al. 1993) of 7×10^{-9} ergs s⁻¹ at the time of detection, “making RE J1255+266 temporarily one of the brightest EUV sources on the sky.” Indeed, Dahlem et al. estimate that the peak WFC S2 filter count rate (after correction for desensitivity following exposure to the Sun) corresponds to about twice the count rate of HZ 43, which is the brightest quiescent source in the EUV sky in this wavelength range (Pounds et al. 1993; Bowyer et al. 1994). An earlier deep (20 ks) WFC S2 filter pointing obtained in 1993 June–July that had included RE J1255+266 in the field yielded no detection of this source; comparing the upper limit to its count rate during this 1993 observation with the observed count rate during the 1994 outburst, Dahlem et al. (1995) conclude that its EUV flux had increased by a factor of at least 7000 at the observed peak of the outburst. The EUV light curve shows an exponential decay with a timescale of slightly less than a day; the rise was not observed.

Dahlem et al. (1995) also summarize the observations at other wavelengths available for RE J1255+266. Simultaneous data from the Burst and Transient Source Experiment (BATSE) on board the *Compton Gamma Ray Observatory* (CGRO) failed to yield a detection, as did earlier observations during the all-sky surveys of the

ROSAT WFC and Position Sensitive Proportional Counter (PSPC) and of the *Extreme Ultraviolet Explorer* (*EUVE*). Of the available radio observations, only the Green Bank survey from 1987 (Gregory & Condon 1991) yielded a significant detection of a source within the WFC error circle of RE J1255+266. The identity of this transient was therefore somewhat mysterious. Based on the available evidence and upper limits, Dahlem et al. judged as unlikely the obvious candidates, such as a BL Lac, blazar, dwarf nova, flare star, or RS CVn. However, they did note the presence of an object with a blue spectrum about 1.3 north-east of the WFC source position in the objective-prism Schmidt plate from the Hamburg Quasar Survey (Engels et al. 1988).

Following some months after the WFC detection of RE J1255+266, Watson et al. (1996) carried out optical observations aimed at identifying its counterpart. They suggested the same blue object (R.A. = 12^h55^m10^s.7, decl. = +26°42′28″; $V = 18.5$) noted by Dahlem et al. (1995) in the Hamburg Quasar Survey plate (it is also present in the Palomar sky survey) based on its unusual optical spectrum, which shows a blue continuum with broad Balmer lines in absorption characteristic of a DA white dwarf, together with very strong and narrow Balmer and He I lines in emission. These and other observations are described in detail by Watson et al. (1996).

Based on their optical spectra, Watson et al. (1996) favor a model in which the DA white dwarf forms the primary of a cataclysmic variable (CV) system with the secondary being a very low mass object. Fitting of the broad Balmer lines enabled them to place some constraint on the white

dwarf parameters and the likely distance of the object.

In 1995 June 7–21 an *EUVE* observation with the Deep Survey (DS) telescope of IN Com, the central star system of the planetary nebula LoTr 5, was made as part of our Guest Observer program. RE J1255+266 lies sufficiently close to IN Com that it is possible to get the former in the field of view of the *EUVE* DS telescope while observing the latter on-axis. Ensuring that the satellite roll angle for our IN Com observation was such that RE J1255+266 was in the field of view of the Lexan/B filter, we were able to obtain an aggregated 137 ks integration of this source. In this paper, we report on our analysis of the resulting data and its impact on the proposed model for the EUV transient of Watson et al. (1996).

2. OBSERVATIONS

IN Com was acquired by the *EUVE* DS telescope on 1995 June 7–21 for an observation that was to last a total of approximately 300 ks of integration time. The *EUVE* DS telescope feeds a three-band EUV spectrometer and an imaging detector with Lexan/B (67–178 Å; 70–185 eV) and Al/C (157–364 Å; 34–79 eV) filters (see, e.g., Bowyer et al. 1994 and references therein for more details on the *EUVE* instrumentation). The DS imager has a field of view of $2^\circ 32'$, which is slightly more than twice the angular distance between IN Com and the reported position of the transient RE J1255+266. During an on-axis observation of IN Com, RE J1255+266 therefore appears in the DS field of view. However, the particular arrangement of the different DS filters means that the satellite roll angle has to be chosen specially in order for a far off-axis source to appear in a particular filter.

Because of the orbit configuration of *EUVE*, an integration time of 300 ks takes about 10 days of elapsed time to accumulate; this is not straightforward to fit into the *EUVE* observing schedule. In the case of IN Com, the observation was interrupted on June 9 and June 15 for short observations of the Moon, and upon its reacquisition, a different satellite roll angle was required. During the first and longer portion of the observation (June 7–15), we ensured that the satellite roll angle was such that RE J1255+266 was in the field of view of the Lexan/B filter. During the second part of the observation (June 15–21), it was in the Al/C filter field. This latter filter is less sensitive than the Lexan/B one, and the Al edge near 170 Å means that its transmission is sharply curtailed at shorter wavelengths. Moreover, the long-wavelength tail of the Al/C filter extends to the geocoronal He II 304 Å line which gives rise to a much higher background than is seen in Lexan/B. Despite the probability, then, that the intrinsic spectrum of RE J1255+266 has more flux within the Al/C filter bandpass than in Lexan/B,

the strong intervening interstellar medium attenuation toward longer wavelengths, coupled with the lower sensitivity and higher background of the Al/C filter, make Lexan/B the filter of choice for attempting to detect RE J1255+266.

The schedule of observations of RE J1255+266 in the Lexan/B and Al/C bandpasses is summarized in Table 1.

3. DATA ANALYSIS

The satellite telemetry corresponding to the time of the IN Com observation was reduced to event list tables and quick position-oriented event files. From these event lists, detector images were created. The first part of our data analysis consisted of very careful visual inspection of the resulting images for any signs of a source at the expected detector location (Fig. 1). The complex off-axis DS point spread function (PSF) renders the application of automated source detection methods extremely difficult. The DS focal plane is curved, while the detector is flat. Consequently, at most detector locations, the PSF is essentially a ring, corresponding to the slight defocus at the detector surface, but vignetted by the three spectrometer grating elements that take three “bites” out of the ring 120° apart. For off-axis sources, this PSF becomes distorted and enlarged. In order to determine the exact shape of the PSF at the expected position of the source, a ray-traced simulation was performed (P. Jelinsky 1997, private communication). Figure 2 shows the results of the simulation overplotted on the detector image: there is no visible excess where the source is expected. We calculated a 3σ upper limit to the count rate of the source using the rectangles in Figure 2 as the “source region” and the area within the circle (excluding the rectangles) as the “background region.” We chose for the source a slightly larger area than the PSF to account for possible detector distortions (which worsen toward the edge of the detector) or small satellite aspect changes and drift. We calculated the effective exposure time excluding all the times in which the observation was affected by high background (e.g., because of passages through the South Atlantic Anomalies) and correcting for instrument dead time, vignetting and telemetry saturation. The effective exposure time for the source in the Lexan/B filter is 137620 s, from which we derived a 3σ upper limit to the count rate of $0.003 \text{ counts s}^{-1}$.

We also performed an experiment based on the ray-trace results to estimate the threshold of visual detection of a source. We attempted to visually ascertain the presence of the source after adding progressively larger numbers of simulated source photons to a blank region of the field having a similar background count rate. We were able to detect a simulated source at the formal 2σ level with some

TABLE 1
EUVE POINTED OBSERVATIONS OF RE J1255+266

Start ^a	End	Effective Exposure ^b (s)	Filter
Jun 7 UT 19:35	Jun 9 UT 22:28	43587	Lexan/B
Jun 10 UT 15:24	Jun 15 UT 18:56	94033	Lexan/B
Jun 15 UT 20:09	Jun 15 UT 22:06	2410	Al/C
Jun 16 UT 16:40	Jun 21 UT 10:40	89542	Al/C

^a All observations were performed in 1995.

^b Effective exposure time corrected for instrument dead time, limited telemetry allocation, and telescope vignetting.

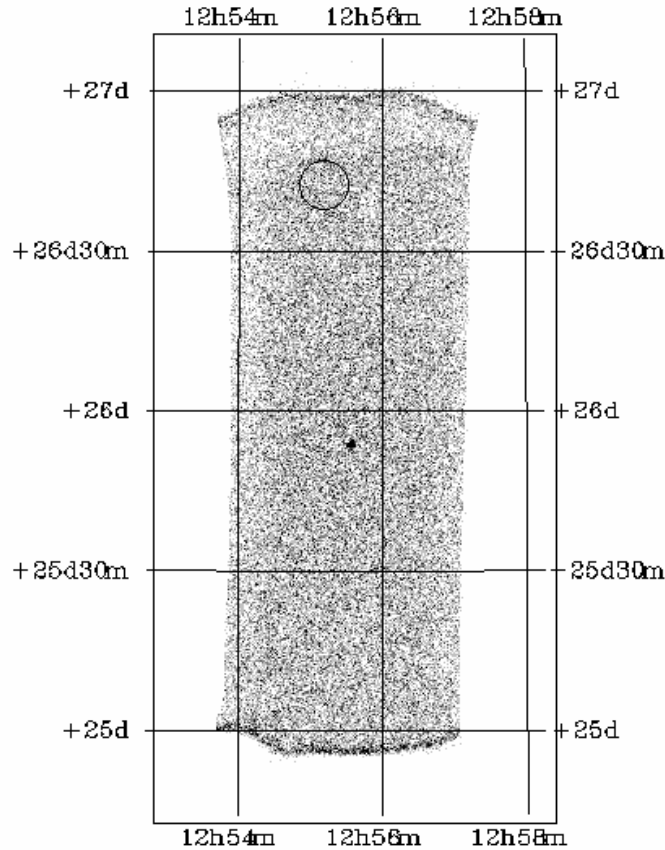


FIG. 1.—The Lexan/B filter of the *EUVE* DS detector for the first two segments of the observation listed in Table 1. The position of the Watson et al. (1996) optical identification of RE J1255+266 is marked; the source was not detected. The bright spot in the detector center is IN Com. The detector edge is discernible by its brighter (black) rim running along arcs at the top and bottom of the image.

confidence, and even at some levels below this. Consequently, we can place an informal upper limit of $0.002 \text{ counts s}^{-1}$ for the source.

This *EUVE* DS observation represents the most sensitive constraint yet obtained on the quiescent EUV emission of RE J1255+266.

4. DISCUSSION

Based on the formal 3σ observed count rate upper limit, we have investigated the parameter space allowed for the source counterpart in order to examine whether or not the identification proposed by Watson et al. (1996) is consistent with this new observation and, furthermore, to investigate the degree to which our observation might place additional constraints on the nature of this object. In this regard, it is also of interest to examine any further constraints provided by the earlier *ROSAT* observations. While the *ROSAT* WFC S2 filter is similar to that of the *EUVE* DS Lexan/B filter and does not provide any additional constraints, the *ROSAT* PSPC has a significantly different bandpass (0.1–2.4 keV) and so might provide some further observational leverage on the nature of the source counterpart. We adopt the count rate upper limit for the PSPC all-sky survey of $0.03 \text{ counts s}^{-1}$ from Dahlem et al. (1995).

4.1. Blackbody Analysis

We have examined the source parameter space firstly using a grid of blackbody model fluxes with a range of

temperatures and normalized in flux so as to match a range of V magnitudes. For each model we have calculated the resulting count rate in the *EUVE* DS and *ROSAT* PSPC instruments, based on the effective area curves of Bowyer et al. (1994) and J. Schmitt (1995, private communication), for a range of different values of the intervening hydrogen column density. The interstellar medium (ISM) opacity was calculated for fixed values of the ratios of the number densities of neutral hydrogen to neutral and once ionized helium of 0.1 and 0.01, respectively.

Firstly, we have calculated the ranges of visual magnitude and temperature allowed by both the DS and PSPC count rate upper limits using a “typical” value for the intervening H I column density. For this “typical” H I column density, we adopted $\log N_{\text{H}} = 19.4$, which was determined by interpolating within the H I column density data of Fruscione et al. (1994) and supplemented by further data culled from the literature by P. Jelinsky (unpublished) for the source direction and the distance of 180 pc determined by Watson et al. (1996) for their proposed source counterpart. The results are illustrated in Figure 3. In this figure, the shaded areas denoted “DS” and “PSPC” to the right of the solid curves denote the parameters that are excluded by the observed upper limits. The horizontal shaded patch to the left of the curves labeled with a “W” corresponds to the visual magnitude and range of its uncertainty of the Watson et al. (1996) identification ($V = 18.0 \pm 0.5$). The placement of the “W” itself indicates the effective temperature of the DA white

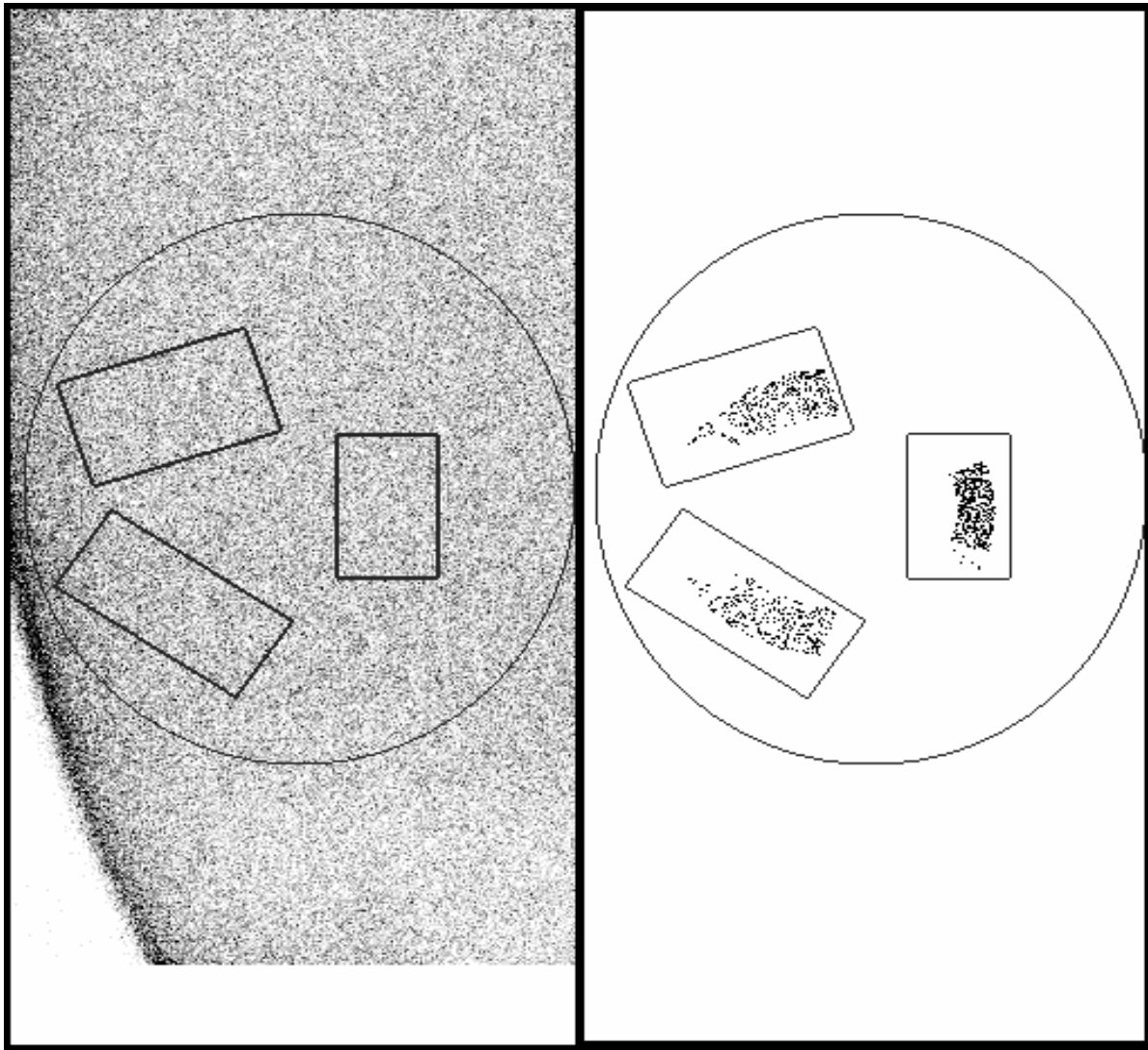


FIG. 2.—The part of the detector of interest enlarged to illustrate the method of determining the upper limit to the count rate of RE J1255+266. The outer boundary of the region of the detector used to determine the background count rate for the Watson et al. (1996) source position is illustrated by the circle, together with the regions used to determine the upper limit to the source count rate (*rectangles*), and the ray-traced illustration of the characteristic trilobed source PSF at this off-axis location.

dwarf proposed as the source primary and determined by Watson et al. (1996) based on its observed Balmer line profiles.

Note that the *EUVE* DS count rate upper limit provides a more stringent limit on the allowed parameters than does the PSPC upper limit within the temperature range corresponding to the V magnitude range we have considered. This is simply due to the fact that the Wien peak lies at longer wavelengths than the respective instrument bandpasses at these temperatures. More important, the Watson et al. (1996) identification lies well within the allowed range of V and T . While DA white dwarf spectral distributions are significantly different to those of a blackbody, especially in the EUV spectral range, this coarse analysis is sufficient to demonstrate that the quiescent flux from the Watson et al. object lies below the detection threshold of existing EUV and soft X-ray observations, assuming that the quiescent emission from any accretion disk present does not contribute significantly at these wavelengths. This conclusion is not altered if heavier elements are present in the white dwarf photosphere at significant abundance levels, since the

strong EUV opacity of heavier elements suppresses flux at short wavelengths, resulting in even lower EUV fluxes for a given effective temperature.

Based on the V magnitude of 18 for the Watson et al. object, we have also examined the dependence of the DS and PSPC count rates on the intervening hydrogen column density. In Figure 4 we illustrate the upper limit in blackbody temperature allowed by the count rate upper limits as a function of neutral hydrogen column density. Note that toward high column densities ($\log N_H \sim 20.4$), the PSPC becomes more sensitive than the DS in that it restricts the allowed blackbody temperature range more. This is of course expected, as the PSPC sensitivity extends up to 2 keV or so, while that of the *EUVE* DS is curtailed shortward of 60 Å or so by its much larger telescope graze angles. Thus, toward high column densities ($\log N_H \sim 21$ or more), the ISM becomes optically thick throughout the *EUVE* DS bandpass.

In Figure 5 we illustrate a similar comparison between the expected DS and PSPC count rates for blackbody models with a range of temperatures for different inter-

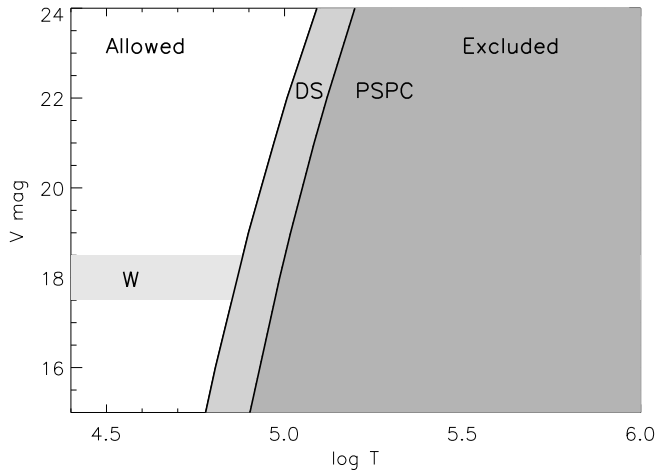


FIG. 3.—Loci corresponding to count rates in the *EUVE* DS and *ROSAT* PSPC instruments of 0.003 and 0.03 counts s^{-1} for blackbody spectra normalized to different V magnitudes and plotted as a function of temperature. The gray areas to the right of the loci are excluded by the DS and PSPC observations because they correspond to count rates higher than the observed upper limits. The shaded area labeled “W” corresponds to the V magnitude range of the identification proposed by Watson et al. (1996); while the location of the “W” corresponds to the DA white dwarf effective temperature. This plot shows that the Watson et al. identification is entirely consistent with the observed upper limits. Calculations were performed for an intervening absorbing column corresponding to a neutral hydrogen column density of $\log N_H = 19.4$ (see text).

vening column densities. The horizontal solid and dashed lines correspond to the observed DS and PSPC upper limits, respectively. Again, we see that the *ROSAT* PSPC becomes more sensitive than the *EUVE* DS toward higher temperatures ($\log T > 5.3$) and at higher column densities.

If the Watson et al. (1996) source identification is correct, it is of interest to determine more accurately the count rate expected by this object in its quiescent phase. To do this, we have calculated the DS count rates for two DA white dwarf model fluxes computed using the non-LTE atmosphere code developed by Koester (e.g., Koester 1991; kindly supplied to us by David S. Finley) and normalized to a visual

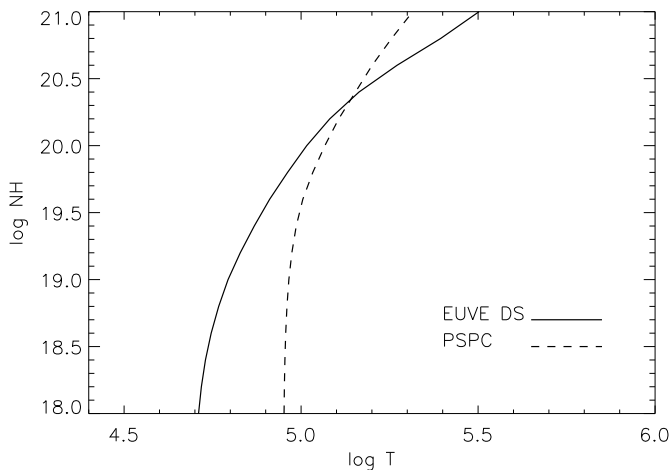


FIG. 4.—Constant count rate loci for blackbody spectra normalized to $V = 18$ in the $\log T$ – $\log N_H$ plane for the observed DS and PSPC 3σ count rate upper limits of 0.003 and 0.03 counts s^{-1} , respectively. As in the previous figure, values to the right of the loci are excluded by the observations. The PSPC upper limit is more sensitive than that of the DS for high column densities of $N_H > 210^{20} \text{ cm}^{-2}$.

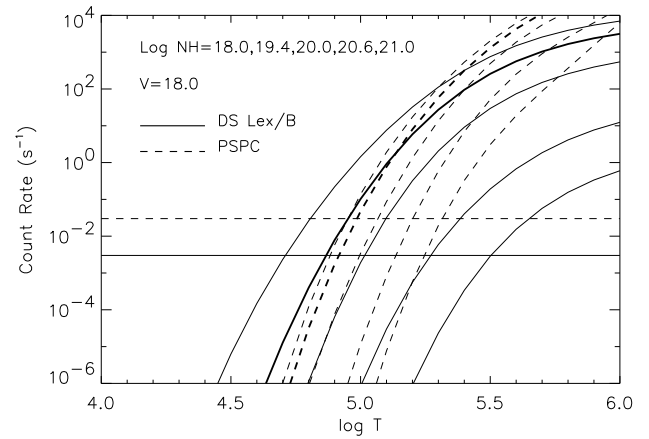


FIG. 5.—Count rates in the DS and PSPC instruments as a function of logarithmic temperature for blackbody spectra normalized to $V = 18$, plotted for different values of the intervening neutral hydrogen column. The respective DS and PSPC upper limits are indicated by the straight horizontal lines.

magnitude of $V = 18$. The model temperatures of 37,000 K and 45,000 K were chosen so as to bracket the best-fit effective temperature and its upper limit uncertainty estimated by Watson et al. (1996); the DS count rate is not very sensitive to the value of surface gravity adopted, and so we have used $\log g = 9.0$ for both models. The expected DS count rates for these models as a function of the intervening H I column density are illustrated in Figure 6 by the solid curves. The shaded regions correspond to the range in count rate caused by the uncertainty in the V magnitude. Our DS count rate 3σ upper limit lies about an order of magnitude above the expected rate.

4.2. Optically Thin Plasma Emission?

We have also investigated the constraints imposed by our observations on the quiescent source emission in the case

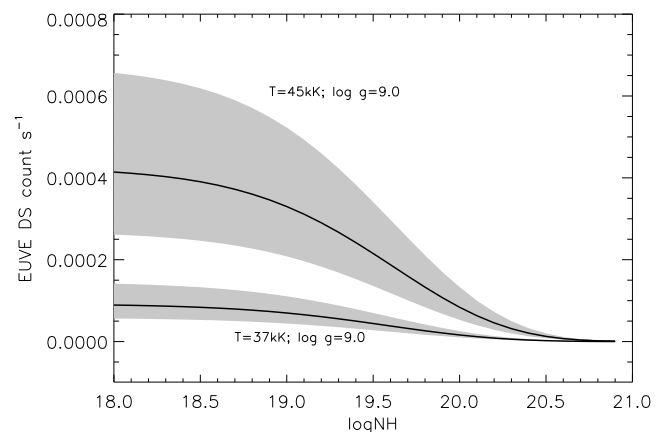


FIG. 6.—*EUVE* DS count rates for two different DA white dwarf pure hydrogen model fluxes calculated using the model atmosphere code of Koester (1991) and normalized to $V = 18$, plotted as a function of intervening neutral hydrogen column density. The different model effective temperatures are to be compared with the value derived by Watson et al. (1996) for the source counterpart primary component of $T_{\text{eff}} = 36840$ with a $\pm 1\sigma$ range of uncertainty of 34,000–42,400 K. The shaded areas correspond to the uncertainty in the V magnitude of ± 0.5 . The count rates for the hotter of the two models are a factor of 5 or so lower than our upper limit of 0.003 counts s^{-1} .

where it can be characterized by an optically thin collisionally dominated plasma. While it appears most likely that the Watson et al. (1996) identification of the source counterpart as a CV-like system renders it improbable that the quiescent emission is akin to that of an optically thin plasma, until the nature of the source is pinned down in more detail such constraints are still of interest.

In Figure 7 we illustrate the optically thin plasma isothermal emission measure solutions that fit the DS and PSPC count rate upper limits; in the case of the DS, we illustrate the curves for several different values of the intervening neutral hydrogen column density. The calculations were carried out using the optically thin plasma loss model of Landini & Monsignori-Fossi (1990). This type of curve is described in detail by Drake (1998) and should be distinguished from the more standard emission measure *distribution* commonly used to describe the distribution of emitting plasma with temperature: it represents the isothermal plasma emission measure that gives rise to a given instrument count rate, plotted as a function of *isothermal* plasma temperature. In the case of multithermal plasmas, these curves then represent the upper limit to the plasma emission measure at any given temperature.

For our “adopted” hydrogen column density of $\log N_H = 19.4$, emission measure upper limits (in units of cm^{-3}) in the range $\log EM < 52\text{--}53$ are indicated for typical coronal temperatures ($\log T \sim 6\text{--}7.5$). Emission measures of this magnitude are similar to those found for the coronae of active RS CVn systems and are not too dissimilar to those found for the most active dMe flare stars. As an example of the latter, the *quiescent EUVE* DS count rate of the dM1e flare star AU Mic of $\sim 0.5 \text{ counts s}^{-1}$ lying at a distance of 9.35 pc corresponds to volume emission measures in the range $10^{52}\text{--}2 \times 10^{53} \text{ cm}^{-3}$ (e.g., Katsova, Drake, & Livshits 1997). The optical data obtained by Watson et al. (1996) rule out a counterpart capable of harboring either a binary companion of the mass and spectral

type (G–K III–V) typical of those found in the RS CVn systems or an early dKe or dMe flare star, and instead a very low mass M dwarf secondary star is indicated by a small excess near-IR flux as compared with a white dwarf model. It is plausible that our *EUVE* DS observation could have detected coronal emission from even an early M dwarf companion if it was sufficiently coronally active. High coronal activity is expected in cases where stars in close binary systems are spun up by tidal forces such that they are rotating synchronously with the system orbital period; examples of this type of system involving M dwarfs are the BY Draconis binaries. However, as stellar mass decreases, so does the coronal luminosity at EUV and X-ray wavelengths (e.g., see the study by Giampapa et al. 1996); our observation is then consistent with a low-mass companion lying toward the low-mass end of the main sequence. An example of such a low-mass M dwarf is the nearby (6.5 pc) dMe star VB 8. The *EUVE* DS count rate for VB 8 observed by Drake et al. (1996) was $0.002 \text{ counts s}^{-1}$; at the distance of the RE J1255+266, the VB 8 count rate would then lie 3 orders of magnitude below our upper limit and 2 or so orders of magnitude below the count rate due to the DA white dwarf. The M dwarf secondary stars of other new close binary DA white dwarf and M dwarf pairs discovered in the EUV (e.g., Cook et al. 1992; Jomaron et al. 1993) were also not detected because of similar contrasts between the late-type stellar coronal emission and the white dwarf photospheric emission.

4.3. Source Brightening Relative to Quiescence

Using our visual count rate upper limit of $0.002 \text{ counts s}^{-1}$, we can estimate the minimum flux contrast between the source in its quiescent state and the peak of the 1994 June–July outburst observed by the *ROSAT* WFC. The peak WFC S2 filter count rate according to Dahlem et al. (1995) was 14 counts s^{-1} in its desensitized state following inadvertent exposure to the Sun, which Dahlem et al. convert to the all-sky survey equivalent count rate of $76.5 \text{ counts s}^{-1}$. In order to compare this with the slightly different bandpass of the *EUVE* DS, we need to assume a spectral model. Following Dahlem et al. (1995) we used an optically thin plasma model (Landini & Monsignori-Fossi 1990) with a temperature of $2 \times 10^5 \text{ K}$, together with our estimated neutral hydrogen column density of $\log N_H = 19.4$, to obtain the count rate conversion factor $DS/S2 = 1.4$. Using this conversion, we find that the source brightened in the EUV at the peak of its outburst by a factor of greater than 54,000 relative to its quiescent state.

5. CONCLUSIONS

A deep 137 ks *EUVE* observation of the field of the *ROSAT* WFC EUV transient source RE J1255+266 carried out in 1995 June with the Deep Survey telescope has failed to yield a detection of the source. The formal 3σ upper limit to the source count rate in the DS telescope Lexan/B filter is $0.003 \text{ counts s}^{-1}$, while a visual upper limit was determined to be $0.002 \text{ counts s}^{-1}$. The formal upper limit, together with the upper limit from the *ROSAT* PSPC all-sky survey, has been used to place constraints on the source counterpart. Sources with spectra approximating that of a blackbody with temperatures $\log T > 5$ are ruled out for V magnitudes $V < 24$ or so. The source counterpart comprising a DA white dwarf in a CV-like system proposed by Watson et al. (1996) is entirely consistent with our

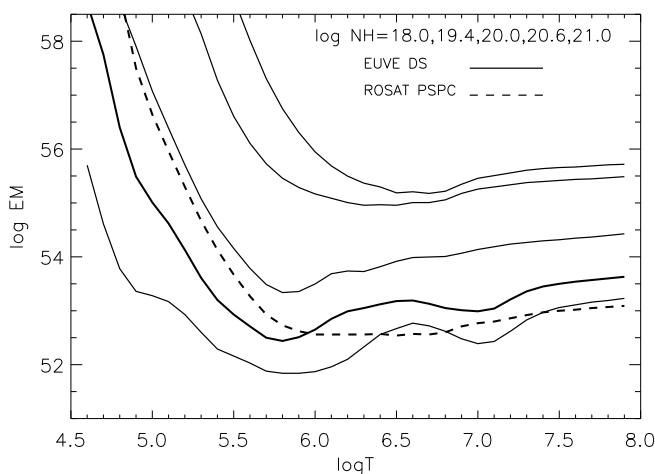


FIG. 7.—Emission measure–temperature loci corresponding to the observed DS and PSPC count rate upper limits; in the case of the DS, we have calculated the loci for different values of the neutral hydrogen column; the PSPC locus (dashed line) was calculated for our “adopted” column of $\log N_H = 19.4$. These curves correspond to the *isothermal emission measure* that would give rise to the count rate upper limits plotted as a function of logarithmic temperature. Note that the DS limit is more sensitive than the PSPC limit only for temperatures below $\log T < 5.9$. The emission measure upper limits are similar to those expected for active RS CVn systems and dKe and early dMe flare stars.

observation; our Lexan/B 3 σ upper limit is an order of magnitude higher than expected from the photospheric emission of the WD. Our upper limit is within the expected count rate range for an early M dwarf secondary star companion spun up to very high coronal activity levels by synchronous rotation with the system orbital period. Our observations then favor a secondary star toward the lower mass end of the M dwarf main sequence, in agreement with the very low mass limits for the secondary star determined by Watson et al. (1996) based on near-IR photometry. Finally, the “visual” count rate upper limit implies a brightening of the source EUV flux by a factor of greater

than 54,000 at the peak of its outburst relative to quiescence.

We would like to express warm thanks to Dr. Patrick Jelinsky for providing ray-trace information for the *EUVE* DS PSF and to Dr. David Finley for supplying the white dwarf model fluxes. J. J. D. and A. F. were supported by AXAF Science Center NASA contract NAS 8-39073 during the course of this work. Finally, we thank Dr. Roger F. Malina and the Center for EUV Astrophysics for providing logistical support for our continuing analysis effort on *EUVE* data.

REFERENCES

- Bowyer, S., Lieu, R., Lampton, M., Lewis, J., Wu, X., Drake, J. J., & Malina, R. F. 1994, *ApJS*, 93, 569
 Cook, B. A., et al. 1992, *Nature*, 355, 61
 Dahlem, M., & Kreysing, H.-C. 1994, *IAU Circ.* 6085
 Dahlem, M., et al. 1995, *A&A*, 295, L13
 Drake, J. J. 1998, in preparation
 Drake, J. J., Stern, R. A., Stringfellow, G. S., Mathioudakis, M., Laming, J. M., & Lambert, D. L. 1996, *ApJ*, 469, 828
 Engels, D., Groote, D., Hagen, H. J., & Reimers, D. 1988, in *ASP Conf. Ser. 2, Optical Surveys for Quasars*, ed. P. S. Osmer et al. (San Francisco: ASP), 143
 Fruscione, A., Hawkins, I., Jelinsky, P., & Wiercigroch, A. 1994, *ApJS*, 94, 127
 Giampapa, M. A., Rosner, R., Kashyap, V., Fleming, T. A., Schmitt, J. H. M. M., & Bookbinder, J. A. 1996, *ApJ*, 463, 707
 Gregory, P. C., & Condon, J. J. 1991, *ApJS*, 75, 1011
 Jomaron, C. M., Branduardi-Raymont, G., Mason, K. O., Naylor, T. T., Hassall, B. J. M., Watson, M. G., Hodgkin, S. T., & Bromage, G. E. 1993, *MNRAS*, 264, 219
 Katsova, M. M., Drake, J. J., & Livshits, M. A. 1997, *ApJ*, submitted
 Koester, D. 1991, in *Proc. IAU Symp. 145, Evolution of Stars: The Photospheric Abundance Connection*, ed. G. Michaud & A. Tutukov (Dordrecht: Kluwer), 435
 Landini, M., & Monsignori-Fossi, B. C. 1990, *A&AS*, 82, 229
 Pounds, K. A., et al. 1993, *MNRAS*, 260, 77
 Watson, M. G., Marsh, T. R., Fender, R. P., Barstow, M. A., Still, M., Page, M., Dhillon, V. S., & Beardmore, A. P. 1996, *MNRAS*, 281, 1016